JOURNAL OF COMPUTATIONAL PHYSICS **141,** 174–198 (1998)
ARTICLE NO. CP985912

Numerical Preservation of Symmetry Properties of Continuum Problems

E. J. Caramana and P. P. Whalen

Hydrodynamic Methods Group, Applied Theoretical and Computational Physics Division, Los Alamos National Laboratory, Los Alamos, New Mexico 87545
E-mail: ejc@lanl.gov

Received April 15, 1997; revised December 24, 1997

We investigate the problem of perfectly preserving a symmetry associated naturally with one coordinate system when calculated in a different coordinate system. This allows a much wider range of problems that may be viewed as perturbations of the given symmetry to be investigated. We study the problem of preserving cylindrical symmetry in two-dimensional Cartesian geometry and spherical symmetry in two-dimensional cylindrical geometry. We show that this can be achieved by a simple modification of the gradient operator used to compute the force in a staggered grid Lagrangian hydrodynamics algorithm. In the absence of the supposed symmetry we show that the new operator produces almost no change in the results because it is always close to the original gradient operator. Our technique thus results in a subtle manipulation of the spatial truncation error in favor of the assumed symmetry but only to the extent that it is naturally present in the physical situation. This not only extends the range of previous algorithms and the use of new ones for these studies, but for spherical or cylindrical calculations it reduces the sensitivity of the results to grid setup with equal angular zoning that has heretofore been necessary with these problems.

1. INTRODUCTION

An outstanding problem in computational physics is the exact preservation of a given one-dimensional symmetry in a coordinate system, distinct from that symmetry. Generally, if one wishes to maintain a given one-dimensional symmetry (cylindrical or spherical, for example) and perform perturbation studies from it in two or three dimensions it is usual to write the problem in terms of that coordinate system at the start. Thus one would

0021-9991/98 $25.00

use cylindrical or spherical coordinates to perform perturbation studies in more than one dimension of problems possessing these symmetries. This makes that symmetry easier to recover in the limit where the initial and boundary conditions, and possibly the energy source terms, are consistent with it. In this paper we investigate the problem of preserving exactly cylindrical or spherical symmetry in Cartesian or cylindrical coordinates, respectively, in two spatial dimensions. If achieved, this allows more flexibility in the study of certain problems, for example in laser fusion applications, than can be attained with the direct use of cylindrical or spherical coordinates.

The organization of this paper is as follows: In Section 2 we give a quantitative explanation of the problem of preserving a one-dimensional symmetry in a coordinate system different from that symmetry. It is shown that the usual control volume scheme is not suitable for this purpose, except for cylindrical symmetry in Cartesian geometry with special, equal-angle, initial zoning. Previous solutions to this problem, all of which are restricted to equal angle initial zoning, are also reviewed. Section 3 presents the major theoretical development wherein we show how the gradient operator that acts on the zone pressure to produce the nodal force can be slightly modified so that the mentioned symmetries are preserved without need to resort to very specialized numerical schemes or with the restriction of equal angle initial zoning. This is done by means of a circle construction through three points that yields a simple formula that enables us to modify the edge vector lengths used in computing the pressure force. The important general idea is that straight lines need not be used to connect coordinate points and that curves of some nature that provide a subtle manipulation of the spatial truncation error can work better. This is done here in a manner that picks out the symmetric solution when present but gives very little difference in the solution when it is not; that difference remains at the truncation error level for a stable difference scheme. The limitations and additional concerns associated with this new form of the pressure gradient operator are given in Section 4. Issues such as the inclusion of an artificial viscosity and additional requirements that must be satisfied for symmetry preservation are discussed. Section 5 presents numerical results intended to validate our claims with regard to the efficacy and accuracy of this new method to achieve the stated goals .The examples are chosen to demonstrate both the ability of the algorithm to capture symmetry when it is present and to still give accurate results when it is absent. The somewhat paradoxical issue of the absence of exact conservation of linear momentum that occurs with methods that preserve symmetry is also discussed. An appendix is included in which the problem of the preservation of symmetry is investigated in the instance when the force is derived from a tensor, as occurs with material strength. Our conclusions are also briefly summarized.

2. STATEMENT OF PROBLEM AND PREVIOUS SOLUTIONS

Consider a staggered grid, Lagrangian, hydrodynamics scheme in which pressure, density, and specific internal energy are centered in the zones and coordinate position and velocity are defined on the points. We are concerned with both (x, y) Cartesian geometry or (r, z) cylindrical geometry as indicated in Fig. 1. There we show an angular distribution of symmetric zonal pressure, with logical k-lines radially outward and logical l-lines in the angular direction forming a quadrilateral grid. We impose reflective boundary conditions on both the horizontal and vertical axes. We are concerned with computing the force due to the symmetric pressure distribution at point "c" defined by the intersection of logical lines

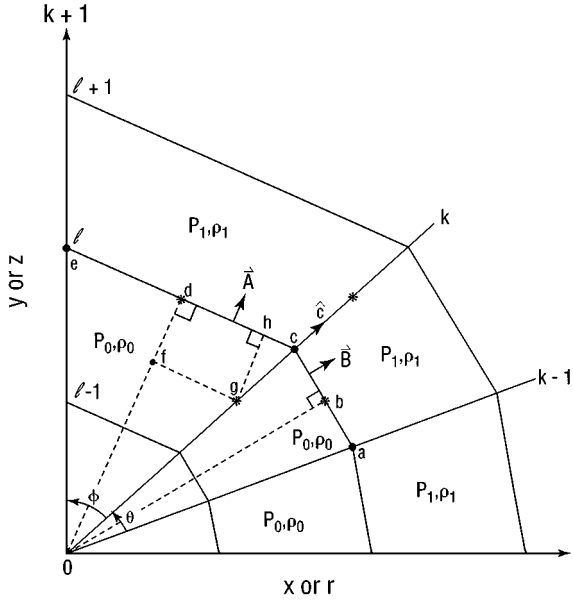

FIG. 1. Unequal angle grid for Cartesian or cylindrical geometry–coordinate line momentum control volume.

(k, l). The logical lines "k," "$k-1$" form an angle θ and those "$k+1$," "k" form an angle ϕ at the origin. Consider for now that we are in (x, y) Cartesian geometry with an ignorable z coordinate pointing out of the page. Then the physical situation shown, with a pressure that has only major radius $R = \sqrt{x^2 + y^2}$ dependence, should only produce radially cylindrical motion. Consider the usual control volume scheme in Cartesian coordinates for computing this force about point "c." A momentum control volume is constructed about this point through the midpoints of the intersecting "k" and "l" lines. These points are indicated by asterisks in Fig. 1. Since the pressure is constant in a zone the force contribution due to that zone at point "c" depends only on the location of these side midpoints. This is conveniently given by the pressure of the zone times the outward normals of the two adjacent intersecting "k" and "l" lines with magnitudes equal to one half of the line segment lengths. We call this the corner force contribution to the point "c" from the given zone. The total force is just the sum of the four corner forces about this point. For the symmetric situation considered here the k-line contributions vanish. Thus defining the outward normal to the two respective l-lines as **A** and **B** with magnitudes equal to the lengths of the half edge line segments $(c-d)$ and $(b-c)$, as shown in Fig. 1, this total force is

$$\mathbf{F}_c = -(P_1 - P_0)\mathbf{A} - (P_1 - P_0)\mathbf{B}. \tag{1}$$

At the point labeled "c" in Fig. 1 we show the unit vector $\hat{c}$ that points along the radial k-line. It is obvious that the force $\mathbf{F}_c$ at this point does not have this same direction unless the vectors **A** and **B** have components normal to $\hat{c}$ that are equal in magnitude and opposite in sign. This will not occur unless the angles θ and ϕ are equal. It is this problem that this paper addresses.

The solution to this difficulty is easily achieved in Cartesian geometry by always zoning this type of problem with equal angle sets of k-lines. This still leaves some concern about sensitivity to source terms that perturb this symmetry since the errors obtained for

unequal angle zoning are quite large, as will be seen. Thus, one worries whether the results of perturbations to this symmetry are real or numerical. In cylindrical geometry where we wish to have spherical symmetry preserved this problem becomes much more severe. Now consider Fig. 1 once again but for cylindrical (r, z) geometry with an ignorable angle coordinate about the z-axis. With all else the same as before and for a control volume scheme in cylindrical coordinates, the force on point "c" becomes

$$\mathbf{F}_c = -(P_1 - P_0)\mathbf{A}\frac{(3r_c + r_e)}{4} - (P_1 - P_0)\mathbf{B}\frac{(3r_c + r_a)}{4}. \tag{2}$$

Because the coordinate lines are revolved about the z axis the surface area includes the r dependent factors seen in Eq. (2) that depend on the coordinates of points "a" and "e" on adjacent k-lines. Since r varies as the cosine of the angle with respect to the r-axis this scheme does not give a force along $\hat{c}$ for the equal angle, or any other angle, zoning. Thus, the popular and usually very effective control volume differencing has been unsuited to this type of problem in cylindrical geometry.

Several techniques have been used in the past to circumvent this difficulty. The most important of these are the so-called "area-weight" differencing and Petrov–Galerkin finite element schemes that have appeared in a number of different forms over the years [1–4]. The basic idea of these schemes is to cast the Cartesian control volume scheme into cylindrical geometry in the very simplest form so that it will still preserve spherical symmetry for equal angle zoning. To this end one gives up the true surface area of an edge and postulates the force on point "c" to be

$$\mathbf{F}_c = -(P_1 - P_0)\mathbf{A}r_c - (P_1 - P_0)\mathbf{B}r_c. \tag{3}$$

Now only a common factor r_c appears in going from Eq. (1) in Cartesian geometry to Eq. (3) in cylindrical geometry. To obtain an acceleration for point "c" we must divide the force with a nodal mass associated with this point. For the area-weight schemes this nodal mass is defined as

$$M_c = r_c(\rho A_{rea})_c, \tag{4}$$

where the quantity $(\rho A_{rea})_c$ is the effective Cartesian inertia associated with point "c." This can be defined in a number of different ways; all of these amount to summing the zone density times some fraction of the zone area (a subzonal area) of all zones surrounding the given point. This fraction is sometimes taken to be one-quarter but can vary between different schemes (cf., Eq. (16)). The important point is that the common factor r_c cancels out on the two sides of the momentum equation giving a force that will be radial for equal angle zoning. The internal energy change caused by these forces is usually calculated using $-PdV$ of a zone, where dV is the change of the cylindrical zone volume in a time step. These schemes have many interesting properties (e.g., points on the z-axis have zero nodal mass but nonzero Cartesian inertia) that are systematically explored elsewhere [4, 5]. (As opposed to area-weight differencing, control volume differencing can be viewed as "volume-weighted.")

Another numerical scheme that has been used to overcome this problem calculates separate accelerations for each edge between two nodes as

$$\mathbf{a}_{edge} = -(P_1 - P_0)\mathbf{B}\frac{(r_a + r_c)/2}{(M_0 + M_1)}. \tag{5}$$

The subscripts "0" and "1" refer to the pressure and mass in the two zones adjacent to any particular edge; here, that is between points "*a*" and "*c*" of Fig. 1. To get the total acceleration on any given point one simply adds together all of the edge accelerations that are associated with that point. This scheme, termed "force gradients" [6, 7], has the potential difficulty that if the initial zonal masses are widely disparate, any magnitude of acceleration can be achieved and no composite form for the discrete gradient operator can be given. This scheme does preserve the desired symmetries in both cylindrical and Cartesian geometry, but only for equal angle zoning.

3. MODIFICATION OF THE GRADIENT OPERATOR

It has been shown that the difficulty in preserving symmetry is due to the difference in the magnitudes of the components of the half-edge vectors **A** and **B** that lie normal to the radial direction $\hat{c}$. It is these normal components that must be modified in some automatic manner such that symmetry will be preserved when it is present in the pressure field and boundary conditions of a physical problem. First, we note that the assumption of connecting nodes by straight lines to form edges that are line segments is not necessary. We could just as well connect them by curves of some form, thus changing the definition of the zone volume. From the Lagrangian assumption of zero flux of mass across these boundaries this effectively changes the discrete form of the divergence operator [5]. However, the difficulty here is not with the definition of the full edge between two nodal points but with the half edges that comprise the gradient operator acting on the zone pressures. We now show how the gradient operator can be modified so that the desired symmetries are preserved for any angle zoning for either the area-weight scheme, Eq. (3), or the cylindrical control volume scheme, Eq. (2), discussed earlier.

Consider a circle constructed through the three points "*a*," "*c*," and "*e*" as given in Fig. 1. We will assume that the origin of this circle lies at point "*o*" without loss of generality since a circle can always be placed through any three points, albeit with infinite radius if collinear. Because of the above assumption the triangles defined by points (*ocdo*) and (*ocbo*) of Fig. 1 are right triangles with opposite sides **A** and **B** to angles $\phi/2$ and $\theta/2$, respectively. We now define a vector

$$\mathbf{W} \equiv a\mathbf{A} + b\mathbf{B}, \tag{6}$$

whose coefficients a and b are to be determined by the requirements that $\mathbf{W} \times \hat{c} = 0$ and whose magnitude is to be equal to $\|\mathbf{A} + \mathbf{B}\|$. The unit vector $\hat{c}$ points from the origin "*o*" to point "*c*" and is the outward normal direction that we require **W** to be parallel to. From the above construction it is apparent that $\|\mathbf{A} \times \hat{c}\| = A \sin(\phi/2)$ and $\|\mathbf{B} \times \hat{c}\| = B \sin(\theta/2)$, where $\sin(\phi/2) = A/R$, $\sin(\theta/2) = B/R$, R is the circle radius (*oc*), A and B are the magnitudes of the respective vectors. Using this in Eq. (6) yields

$$\mathbf{W} = \left(\frac{B}{A}\mathbf{A} + \frac{A}{B}\mathbf{B} \right). \tag{7}$$

Since it is the direction of **W**, defined as $\hat{w}$, that lies parallel to $\hat{c}$ when symmetry is present we have that

$$\hat{w} = \hat{c} = \frac{B^2\mathbf{A} + A^2\mathbf{B}}{\|B^2\mathbf{A} + A^2\mathbf{B}\|}. \tag{8}$$

In symmetric flow, where we have the same pressure difference $(P_1 - P_0)$ across the sides **A** and **B** we require that the total force act in the direction $\hat{w}$ and on an area $\|(\mathbf{A}+\mathbf{B})\cdot\hat{w}\|$ which, as we shall show, matches the magnitude of the nodal mass to within factors that are independent of angle so that the acceleration will have a magnitude constant along an l-line. We arrange this by modifying the vectors **A** and **B** so that their components normal to $\hat{w}$, as given by Eq. (8), cancel while using $\hat{w}$ as a projection operator to select their parallel components and leave them unchanged. To this end we define

$$\mathbf{A}_\perp \equiv \mathbf{A} - (\hat{w}\cdot\mathbf{A})\hat{w}, \tag{9}$$

$$\mathbf{B}_\perp \equiv \mathbf{B} - (\hat{w}\cdot\mathbf{B})\hat{w}, \tag{10}$$

$$\mathbf{C}_\perp = (\mathbf{A}_\perp - \mathbf{B}_\perp)/2. \tag{11}$$

We have substracted the normal component of **B** from that **A**, since these are always of opposite sign, and simply averaged them to obtain $\mathbf{C}_\perp$, which becomes the modified normal component of **A**. We now add and substract this vector to the unchanged parallel components of **A** and **B** to obtain the modified half-edge vector lengths of the new gradient operator, $\mathbf{A}_m$ and $\mathbf{B}_m$, as

$$\begin{aligned}\mathbf{A}_m &= (\mathbf{A}\cdot\hat{w})\hat{w} + \mathbf{C}_\perp \\ &= \frac{1}{2}([(\mathbf{A}+\mathbf{B})\cdot\hat{w}]\hat{w} + (\mathbf{A}-\mathbf{B})), \\ &= \mathbf{A} - \frac{1}{2}(\mathbf{A}_\perp + \mathbf{B}_\perp),\end{aligned} \tag{12}$$

$$\begin{aligned}\mathbf{B}_m &= (\mathbf{B}\cdot\hat{w})\hat{w} - \mathbf{C}_\perp \\ &= \frac{1}{2}([(\mathbf{A}+\mathbf{B})\cdot\hat{w}]\hat{w} - (\mathbf{A}-\mathbf{B})), \\ &= \mathbf{B} - \frac{1}{2}(\mathbf{A}_\perp + \mathbf{B}_\perp),\end{aligned} \tag{13}$$

from which it follows immediately that

$$(\mathbf{A}_m + \mathbf{B}_m) = [(\mathbf{A}+\mathbf{B})\cdot\hat{w}]\hat{w}, \tag{14}$$

if the pressure distribution is symmetric. Note that we obtain the identity transformation if either $\mathbf{A}_\perp = -\mathbf{B}_\perp$, which is the case along l-lines for equal angle k-line zoning in Cartesian geometry, or for $\mathbf{A}_\perp$ and $\mathbf{B}_\perp$ individually zero, as is the case along the straight k-lines shown in Fig. 1.

Now the force as given by either Eq. (1) for Cartesian geometry or Eq. (3) for the area-weight scheme in cylindrical geometry is unchanged except that the vector half-edge lengths $\mathbf{A}_m$ and $\mathbf{B}_m$ are used in place of **A** and **B**. For the force defined by Eq. (2) for a control volume scheme in cylindrical geometry, the direction vector $\hat{w}$ in Eq. (8) is defined with vectors **A** and **B** as above. However, in the modification procedure Eqs. (9)–(13) the edge vectors are the true surface areas so that $\mathbf{A}' \equiv \mathbf{A}(3r_c + r_e)/4$ and $\mathbf{B}' \equiv \mathbf{B}(3r_c + r_a)/4$ are used in place of **A** and **B**. With $\mathbf{A}'_m$ and $\mathbf{B}'_m$ defined in this manner the force for the control volume scheme in cylindrical geometry has the form given by Eq. (1).

By using Eq. (8) to directly rearrange the transformation given by Eqs. (12)–(13) this can be more elegantly written in matrix form as

$$\begin{pmatrix} \mathbf{A}'_m \\ \mathbf{B}'_m \end{pmatrix} = \begin{bmatrix} 1+\alpha & -\beta \\ \alpha & 1-\beta \end{bmatrix} \begin{pmatrix} \mathbf{A}' \\ \mathbf{B}' \end{pmatrix}, \tag{15}$$

where

$$\begin{aligned} \alpha &= \frac{(BB' - AA')}{2W^2}(1 + \mathbf{A}\cdot\mathbf{B}/A^2)\frac{A}{A'}, \\ \beta &= \frac{(BB' - AA')}{2W^2}(1 + \mathbf{A}\cdot\mathbf{B}/B^2)\frac{B}{B'}, \\ W^2 &= A^2 + B^2 + 2\mathbf{A}\cdot\mathbf{B}. \end{aligned}$$

For either the control volume scheme in Cartesian geometry or for the area-weight scheme in cylindrical geometry the factors of "r" become equal to unity and $\mathbf{A}' \to \mathbf{A}$, $\mathbf{B}' \to \mathbf{B}$ in the above transformation that now holds for all cases Eqs. (1), (2) and (3).

Next we show that the nodal mass has the dependence $\|(\mathbf{A}+\mathbf{B})\cdot\hat{w}\|$ when symmetry is present so that the acceleration of different (k, l) points along a given l-line in Fig. 1 have the same constant magnitude. Consider the corner area (*cdfgc*) shown in Fig. 1. This area has been divided into two pieces: the rectangle (*ghdfg*) and the right triangle (*gchg*) that is similiar to the right triangle (*ocdo*). Defining R as the major radius length (*oc*) on which the points "*a*," "*c*," and "*e*" lie, (*gc*) as the length between points "*g*" and "*c*," and using the fact that $(ch)/(cd) = (gc)/R$, this corner area is given by

$$AREA_{(cdfgc)} = \mathbf{A}\cdot\hat{c}[(gc) - (gc)^2/(2R)]. \tag{16}$$

Since $\hat{c} = \hat{w}$, this is the expression we seek. Similiar formulas hold for the other three corner masses so that the angle-dependent quantity $\|(\mathbf{A}+\mathbf{B})\cdot\hat{w}\|$ appears in composite form, cancelling with a like piece in the total force on a node and resulting in an acceleration that is radial in direction with a magnitude that is constant along any given l-line. This argument also holds for the control volume scheme in cylindrical geometry, where the corner volumes are more complicated to compute.

So far we have concentrated only on the force contributions across l-lines, since for a symmetric pressure distribution the k-lines contribute zero. For a problem without any given symmetry the k-lines give a nonzero contribution to the acceleration of the node. We thus modify the half-edge lengths along the k-line at point "*c*," with coordinates (k, l), in exactly the same manner as for the l-line given above. That is, we define a new $\hat{w}$ based on the half-edge k-line lengths and proceed as before. For the case of straight lines as shown in Fig. 1 this results in no change in this portion of the gradient operator since $\hat{w}$ as determined from Eq. (8) will turn out to be normal to the k-line. Thus we have found an automatic procedure for modifying the gradient operator that consists of independent sweeps along logical "k" and "l" lines wherein the half-edge area vectors that define this operator are slightly modified. For a quadrilateral we now have eight independent vector lengths instead of the usual four. For the case of points on an outer boundary (an l-line boundary in Fig. 1), where we have only two points for the k-line part of the gradient modification, or for other exceptional points where the character of the grid departs from a logical structure, we simply omit this procedure and leave these pieces of the gradient operator unchanged.

In the case where the grid departs from a logical structure, symmetry may not be obtainable even in principle. Consider the grid as shown in Fig. 1 and suppose that we modify this grid by allowing either a k-line or an l-line to terminate at some interior point. To be specific suppose that the segment $(c - e)$ is omitted from the line labelled as "l." Then at the point "c," where this line terminates, one has pressures P_1 and P_0 to the right of the line labelled "k," but the pressure of the newly formed zone to the left of this line can obviously not have either of these values and must be some average of the two. The forces perpendicular to the outward major radial direction cannot now possibly be zero and symmetry cannot be preserved. That is, the grid topology in this instance does not allow for the existence of a symmetric distribution of pressure and perfectly symmetric flow is fundamentally excluded. Now suppose that the line labelled as "k" in Fig. 1 terminates at point "c" and does not continue to the origin "o." (This is useful to prevent highly elongated zones near a center of convergence and a resulting unphysical decrease in timestep.) In this case a symmetric distribution of pressure is still possible and thus symmetric flow is still obtainable in principle. However, to achieve this requires a very careful examination of both the forces and masses that are associated with the now exceptional point "c."

4. ADDITIONAL CONSIDERATIONS

In addition to defining the discrete gradient operator along coordinate lines, another way to represent it is via the median mesh construction shown in Fig. 2 about point "c." There we show eight normal vectors to line segments that connect side midpoints to zone centers, the latter defined as the average of the coordinates of the zone points. The corner force associated with the lower right-hand zone that acts on point "c" is $-P_0(\mathbf{S}_1 + \mathbf{S}_2)$, or equivalently, $P_0(\mathbf{B}_1 + \mathbf{B}_2)$ if written along coordinate lines. As mentioned earlier, the

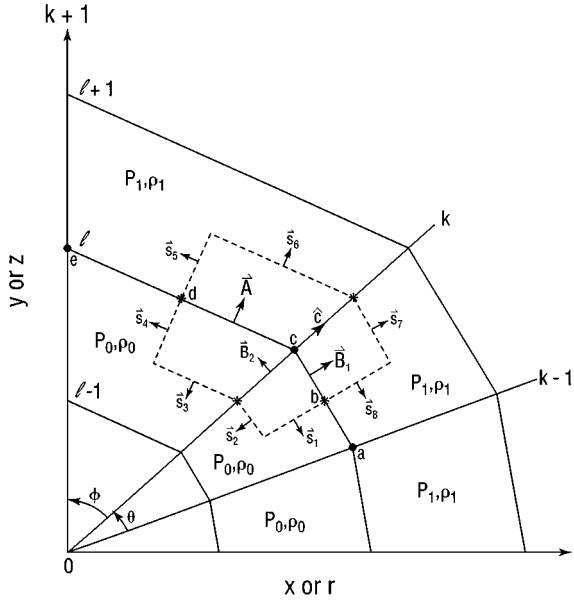

FIG. 2. Unequal angle grid for Cartesian or cylindrical geometry–median mesh momentum control volume.

sum of these corner forces about point "c" will result in the total force $\mathbf{F}_c$ as given by Eqs. (1)–(3), where for the area-weight scheme a factor of r_c is inserted and for the cylindrical control volume scheme, Eq. (2), the lengths $\mathbf{S}_i$ have coordinate factors, r, already included. (These are always the average of r at the two defining endpoints of these eight segments.) Before gradient modification, the coordinate line and median mesh representations of the gradient operator are identical. However, we cannot transform the modified form given along coordinate lines to the median mesh and thereby obtain a median mesh representation of the pressure force that will preserve symmetry. To see this consider the four relations that connect the four median mesh, $\mathbf{S}_i$, of a zone to the four original edge vectors, $\mathbf{B}_i$, of the same zone, one of which is $\mathbf{S}_1 + \mathbf{S}_2 = -(\mathbf{B}_1 + \mathbf{B}_2)$. Because of the hourglass motion associated with a quadrilateral grid [8] the matrix of this transformation is singular and it is thus not possible to invert this relation to obtain the $\mathbf{B}$'s solely in terms of the $\mathbf{S}$'s. So the new gradient operator defined with respect to the coordinate lines cannot be directly transformed to the median mesh.

We next ask whether or not the procedure used along coordinate lines can simply be used directly to modify the gradient operator along the median mesh to obtain symmetry. That is, we use Eq. (8) to define independent $\hat{w}$ directions for the pairs of lengths $(\mathbf{S}_2, \mathbf{S}_3)$, $(\mathbf{S}_4, \mathbf{S}_5)$, etc. and to proceed as before. This will work fine for the pairs $(\mathbf{S}_2, \mathbf{S}_3)$, $(\mathbf{S}_6, \mathbf{S}_7)$; however, the pairs $(\mathbf{S}_1, \mathbf{S}_8)$, $(\mathbf{S}_4, \mathbf{S}_5)$ are collinear and this procedure results in no change in the portion of the gradient operator due to these lines. This presents a problem since the piece of force $-P_0(\mathbf{S}_1 + \mathbf{S}_4)$, or $-P_0(\mathbf{S}_5 + \mathbf{S}_8)$, is not in the radial direction and these contributions do not individually vanish. Thus the median mesh is not appropriate, in general, for gradient operator modification. However, this is still a very useful procedure when subzonal pressures are introduced into a quadrilateral zone [9]. Then with an appropriate representation of the pressure forces (they are decomposed into zone mean and perturbed contributions) these pairs that cause difficulties here will not contribute, and symmetric flow with subzonal pressure forces can be achieved by utilizing a combination of the median and coordinate line meshes in the force differencing. The definition and treatment of these forces is given elsewhere [9].

It is not enough to specify a symmetric nodal acceleration in the radial direction to obtain the desired symmetry. The work done by the forces associated with that acceleration must also yield a symmetric specific internal energy in zones with different volumes so that a symmetric zonal pressure distribution is maintained in time. For the procedure given here this is the case. We can evolve the specific internal energy equation with either $-P\,dV$ heating or by means of compatible heating [5]. In the latter case the new gradient operator defines a new divergence operator. For the case of symmetric flow this is without error, and for other flows it shows little significant difference from the unmodified form, as will be seen by the examples.

For convergent shock wave problems, as opposed to simple adiabatic expansion, we need to include some form of artificial viscosity. If we use a scalar artificial viscosity, q, that enters just like a pressure but turns off in an expanding zone, then as long as q does not depend on any zone scale lengths it will have the same symmetry properties as the pressure field. (The q in [1] is an example of this.) Then replacing P with $(P + q)$ will suffice. However, a scalar q that depends on zone scale lengths will generally violate symmetry requirements and is not suitable [10]. A simple scalar form for q can give very poor results, particularly on problems where a distinction between shock and adiabatic compression is needed. We have developed an edge-centered artificial viscosity that is independent of

grid parameters. This is used for the numerical calculations presented here. It has a simple tensor form and both a linear and a nonlinear part. It requires no special treatment to satisfy symmetry conditions and is superior to scalar forms [11].

5. NUMERICAL RESULTS

In this section we show two sets of numerical examples with a twofold purpose. First, we wish to demonstrate the effectiveness of the new gradient operator to preserve the aforementioned symmetries for the area-weight scheme with unequal angle zoning and for the control volume scheme in cylindrical geometry for any angle zoning. Second, we wish to demonstrate that the new gradient operator causes very little change in the results when no symmetry is present in a given problem. All problems are run with an ideal gas, $\gamma = 5/3$, equation of state. Heating is done compatibly with total energy conserved to roundoff error [5].

We begin by considering the implosion problem of Lazarus [12], Guderley [13], and Stanyukovich [14] for which there is a self-similiar solution. A sphere of unit initial radius with zero specific internal energy and unit density is driven by an inward radial velocity given in good approximation by

$$\mathbf{V}_R(t) = \frac{-\alpha f}{(1 - ft)^{1-\alpha}} \tag{17}$$

where $\alpha = 0.6883545$, $f = 1. - \epsilon t - \delta t^3$, $\epsilon = 0.185$, and $\delta = 0.28$. We use a grid of four k-lines and 201 l-lines.

Figure 3a shows the grid using equal angle initial zoning and area-weight differencing at a time $t = 0.80$ after the shock wave has reflected from the center of convergence and is moving outward into the already shocked medium. Symmetry is preserved as expected for this scheme. In Fig. 3b we show results for this problem with the original gradient operator using the control volume scheme with equal angle initial zoning in cylindrical geometry at $t = 0.73$ shortly before the code quits due to excessive grid distortion. This is due to the fact that this scheme does not preserve spherical symmetry in cylindrical geometry and shows why it has not been widely used to compute nearly spherical flow problems. In Fig. 3c we show the grid for this problem utilizing the new gradient operator with the otherwise identical control volume scheme in cylindrical geometry at $t = 0.8$, after the shock wave has reflected off the origin. Symmetry is preserved to roundoff error, about 10 decimal digits in both the density and specific internal energy on a 64-bit computer, just as precisely as in Fig. 3a using area-weight differencing. In Fig. 3d we show the density versus the major radius at three different times, $t = 0.74, 0.75, 0.80$ as the dashed curves, as well as the analytic solution at $t = 0.74, 0.80$ as solid curves. The shock wave arrives at the origin just after $t = 0.75$, and at this time the density should be flat. The numerical results are seen to lag in time by a small amount relative to the analytical solution; this decreases as more l-lines are added.

Results of this problem using unequal angle initial zoning for area-weight and control volume differencing, both with the modified pressure gradient operator, are given in Fig. 4. The initial grid consists of k-lines at 0°, 18°, 27°, and 90° with respect to the r-axis. The grid at time $t = 0.80$ is displayed in Fig. 4a and in Fig. 4b using modified area-weight and modified control volume differencing, respectively. These results are almost identical. Symmetry is preserved to roundoff error. The density as a function of major radius along a

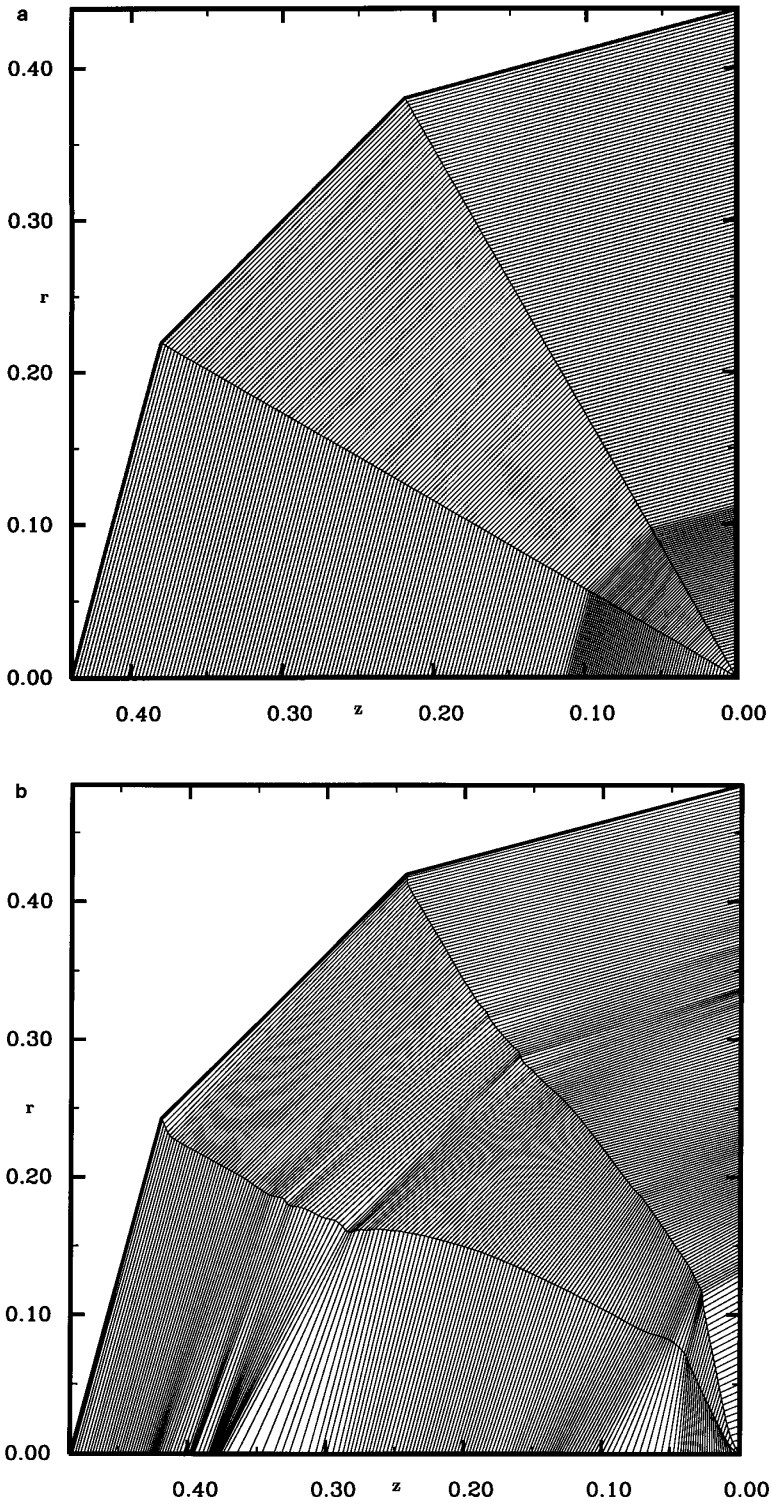

FIG. 3. (a) Lazarus implosion problem with equal angle zoning. Grid at $t = 0.80$ using the area-weight scheme—original gradient operator. (b) Lazarus implosion problem with equal angle zoning. Grid at $t = 0.73$ using the control volume scheme—original gradient operator. (c) Lazarus implosion problem with equal angle zoning. Grid at $t = 0.80$ using the control volume scheme—new gradient operator. (d) Lazarus implosion problem with equal angle zoning. Density versus major radius at $t = 0.8, 0.75, 0.74$ using the control volume scheme—new gradient operator. Dashed lines are numerical solution, solid lines are known solution.

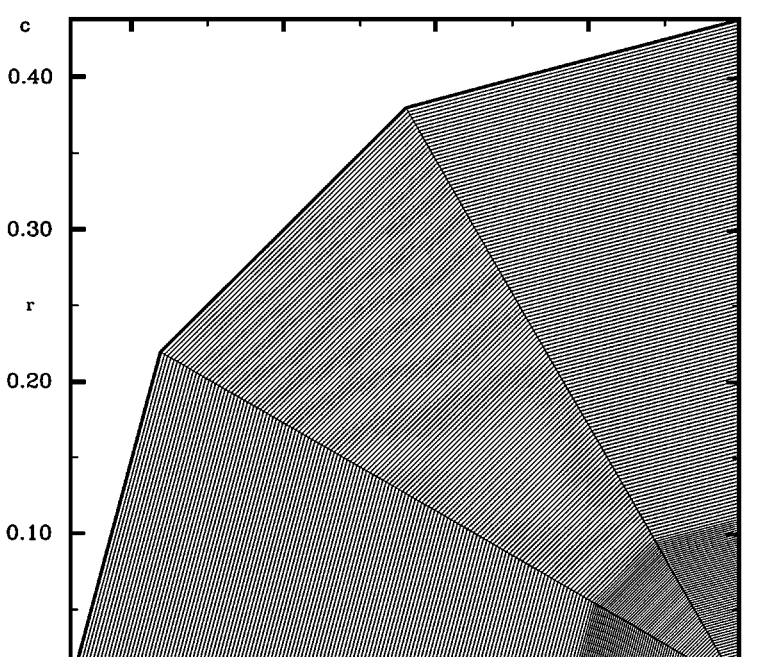

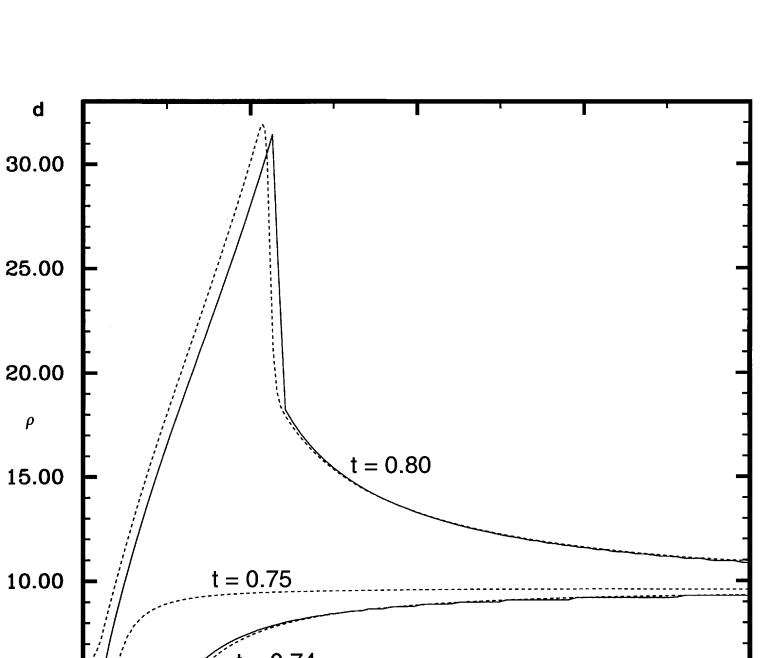

FIG. 3—*Continued*

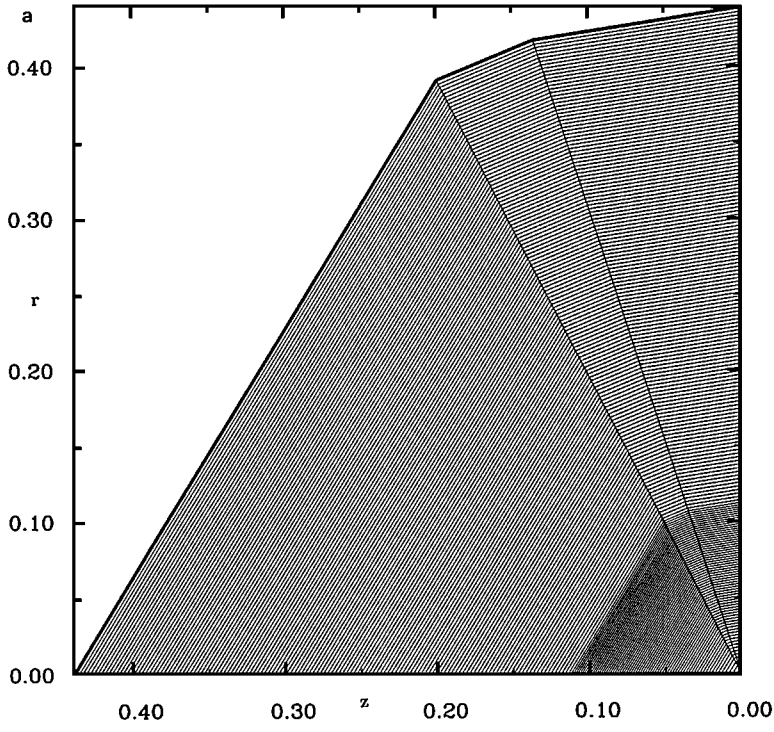

FIG. 4. (a) Lazarus implosion problem with unequal angle zoning. Grid at $t = 0.80$ using the area-weight scheme—new gradient operator. (b) Lazarus implosion problem with unequal angle zoning. Grid at $t = 0.80$ using the control volume scheme—new gradient operator. (c) Lazarus implosion problem with unequal angle zoning: density versus major radius. Solid curve–modified area-weight scheme, all k-lines. Dashed curve–modified control volume scheme, all k-lines.

k-line is shown in Fig. 4c, where the dashed line is the result using modified control volume differencing; the result for area-weight differencing is the solid line that has a slightly lower peak value. Although six curves are actually drawn, only the single solid and dashed lines are visible since the separate sets of three agree to within 10 decimal digits. With this initial grid the code will crash very early in the run for any scheme without the new gradient operator; therefore, these results are not displayed.

The following set of examples is aimed at showing that where symmetry is not present the new gradient operator does not impose it and, in addition, gives results very similiar to that obtained with the unmodified form. We begin with an aspherical expansion problem in cylindrical geometry [15]. The initial conditions are a sphere with 11 equal angle k-lines and 101 l-lines with a major radius equal to 10. The specific internal energy is constant at 0.9, but the initial density profile is given as

$$\rho(t = 0) = \exp -0.5((z/2)^2 + (r/8)^2). \tag{18}$$

Reflective boundary conditions are applied on the "r" and "z" axes but the outermost l-line is a free boundary with zero exterior pressure. The higher density along the r-axis results in an aspherical expansion of the initially spherical grid. In Figs. 5a, b we show the grid and a contour plot of the density at $t = 10.0$ using the area-weight scheme with an unmodified gradient operator. For comparison the same results are given in Figs. 5c, d with the new gradient operator. These results are seen to be almost identical.

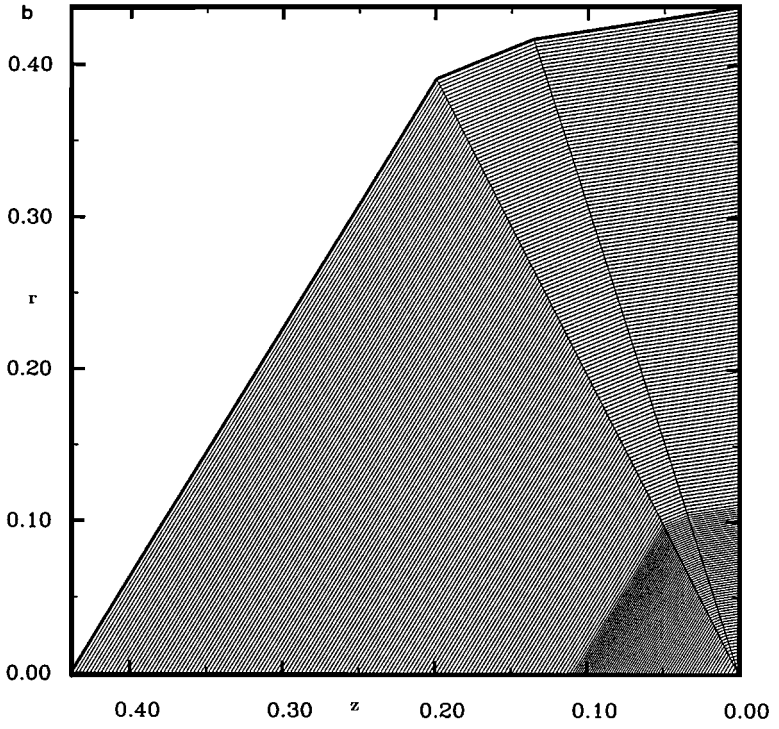

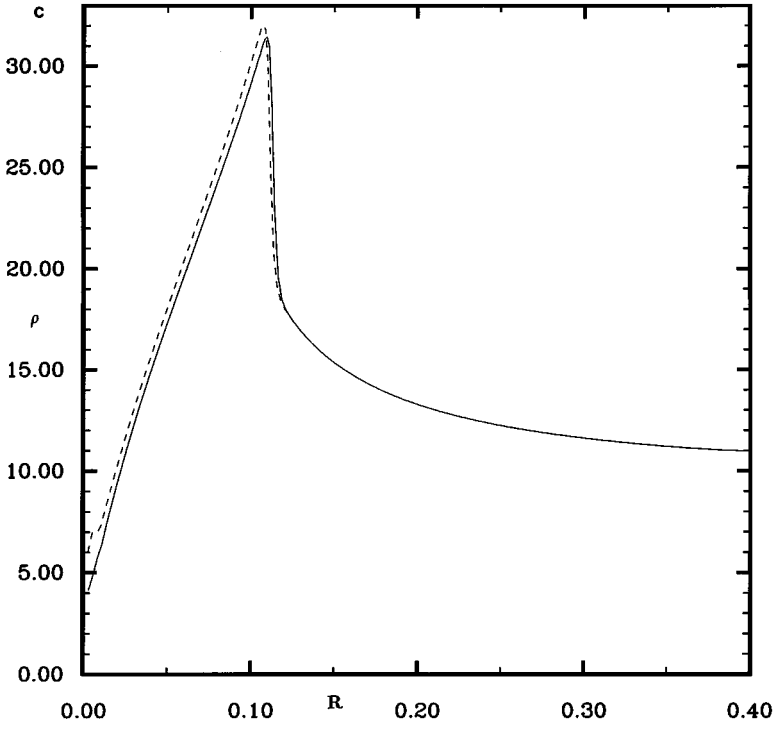

FIG. 4—*Continued*

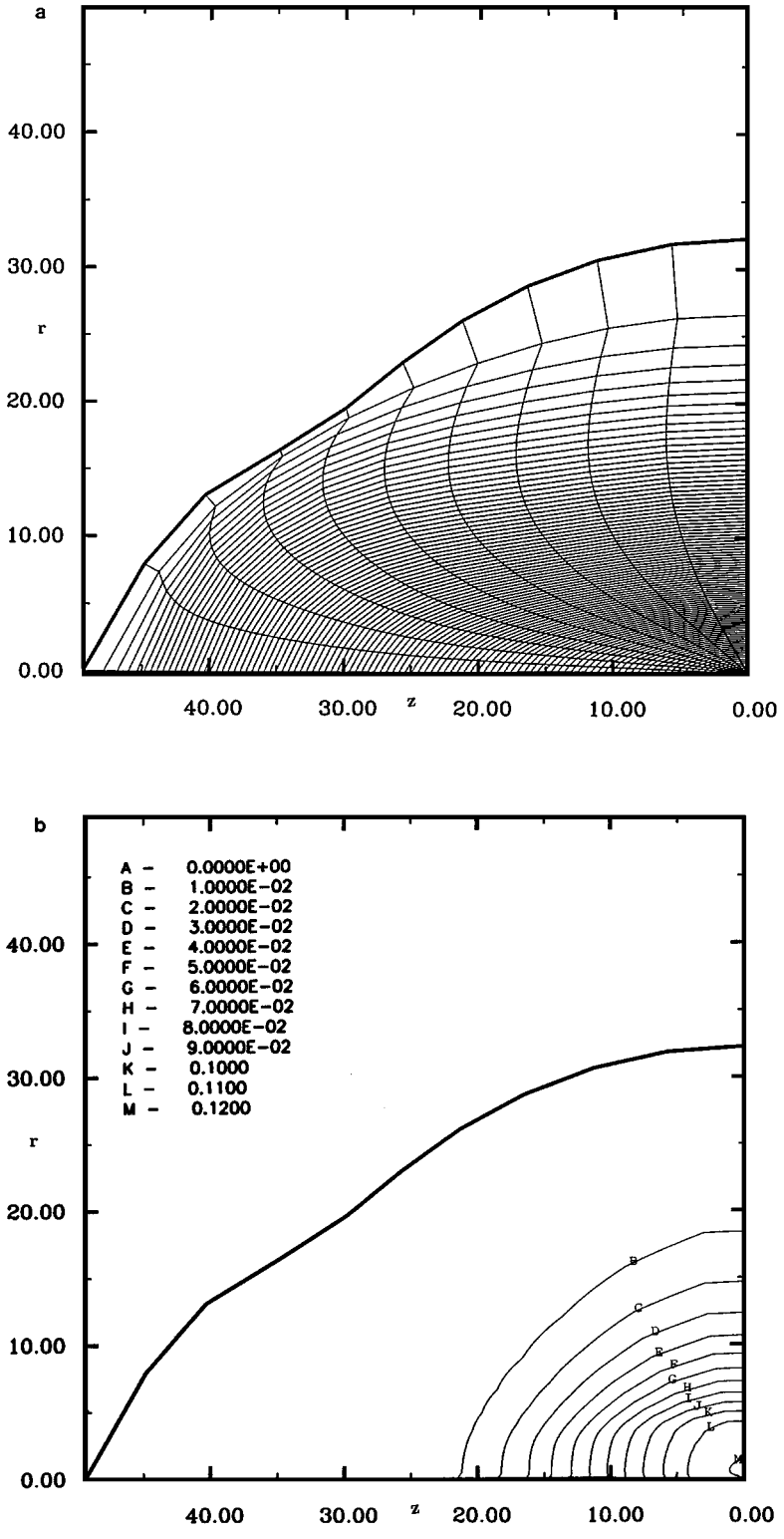

FIG. 5. (a) Aspherical expansion problem. Grid at $t = 10.0$ using the area-weight scheme with original gradient operator. (b) Aspherical expansion problem. Contour plot of density at $t = 10.0$ using the area-weight scheme with original gradient operator. (c) Aspherical expansion problem. Grid at $t = 10.0$ using the area-weight scheme with new gradient operator. (d) Aspherical expansion problem. Contour plot of density at $t = 10.0$ using the area-weight scheme with new gradient operator.

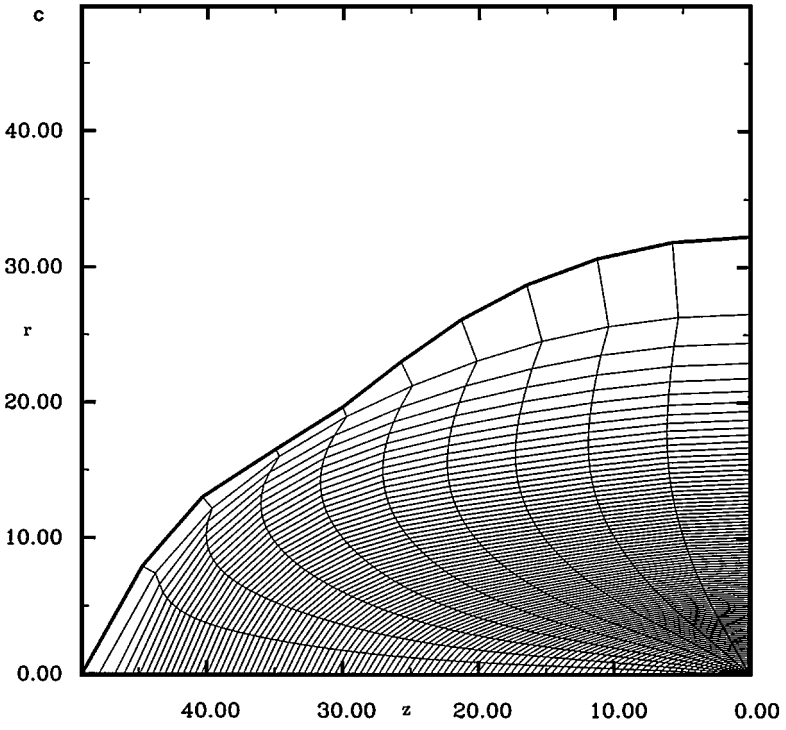

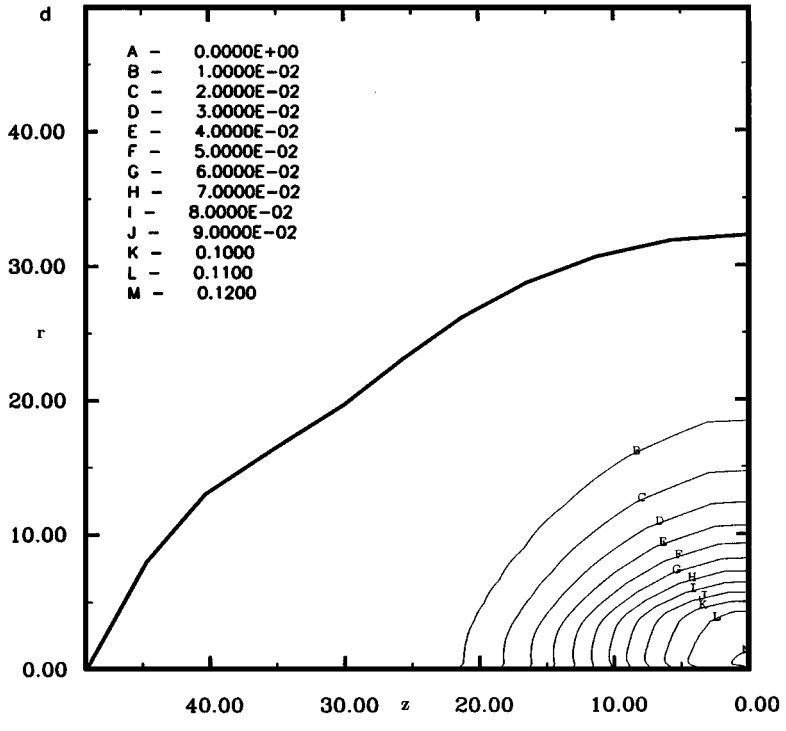

FIG. 5—*Continued*

Next we consider the Saltzman piston problem in cylindrical geometry [8, 16]. This test problem is commonly used to access the difficulties of grid tangling and spurious vorticity [8, 9, 16]. It consists of 101 k-lines dividing the unit z interval and skewed in the radial direction with a half wavelength sinwave dependence, and 11 l-lines uniformly spaced on a radial interval of 0.1 in length so that the initial zones have unit aspect ratio. The grid coordinates are thus given by

$$r_{k,l} = 0.01 * (l - 1),$$
$$z_{k,l} = 0.01 * (k - 1) + 0.01 * (11 - l) * \sin(0.01 * \pi(k - 1)).$$

Reflective boundary conditions are specified at $r = 0.0$ and at the upper boundary $r = 0.10$. These are applied in two different ways. At $r = 0.0$ we reflect both the coordinates and the velocity of the $l = 2$ line about the z-axis so that $r = 0$ corresponds to the center of these zones. Thus, there are no dynamical points on the z-axis. This type of implementation of a reflective boundary condition sometimes yields superior results relative to the more usual case where dynamical points are placed on the axis of symmetry [5]. At the upper boundary $r = 0.1$ we simply set the radial velocity equal to zero in the more standard implementation of this boundary condition. A piston with unit velocity from the right drives a shock into a cold medium with unit density. Figures 6a, b show the grid and a contour plot of the density at $t = 0.80$ after the shock has hit the fixed wall at $z = 1.0$ and has bounced part way back toward the moving piston. The control volume scheme with the unmodified gradient operator was used; the density should be 4.0 and 10.0 in the two regions and is close to these values. In Figs. 6c, d these same plots are shown using the new gradient operator. The differences between these results are again seen to be very small. In both calculations shown in Fig. 6 subzonal corner pressures have been utilized [9].

The above piston problem run on a purely rectangular initial grid, as opposed to the skewed grid of Fig. 6, has been of much importance in the development of the new gradient operator given in this paper. In this case the velocity components that are perpendicular to $\hat{w}$ are at the level of roundoff error for both k-lines and l-lines. It was found that if these perpendicular components are simply set to zero, instead of being made equal in magnitude, that an extremely virulent hourglass-type pattern develops from roundoff error noise in regions that are behind the moving shock; this destroys the solution. Thus these perpendicular components are restored not only to make the new gradient operator as close as possible to the old one and still preserve symmetry, but also to prevent an enhanced sensitivity to spurious hourglass-type motions from occurring.

A wide range of cases, in addition to those shown here, have been run with the new gradient operator versus the old for problems that either have no symmetry or with symmetry but using initial grids not oriented along the symmetry direction, and only small differences have been observed. We have thus demonstrated that the new gradient operator produces changes that are minor, wherein the differences remain at the spatial truncation error level, when used on problems that are nonsymmetric. In fact, it is easy to see for a grid as shown in Fig. 1, but with equal angle zoning, that if a $2\delta\theta$ perturbation is applied to any given l-line, the $\hat{w}$ direction calculated from Eq. (8) remains radial. Thus the gradient operator is not changed for this type of high spatial scale perturbation. We have noticed for problems where the grid is allowed to become highly distorted, and where accuracy is lost anyway, that sometimes more code robustness in terms of runtime can be achieved with the original unmodified gradient operator, all else being equal.

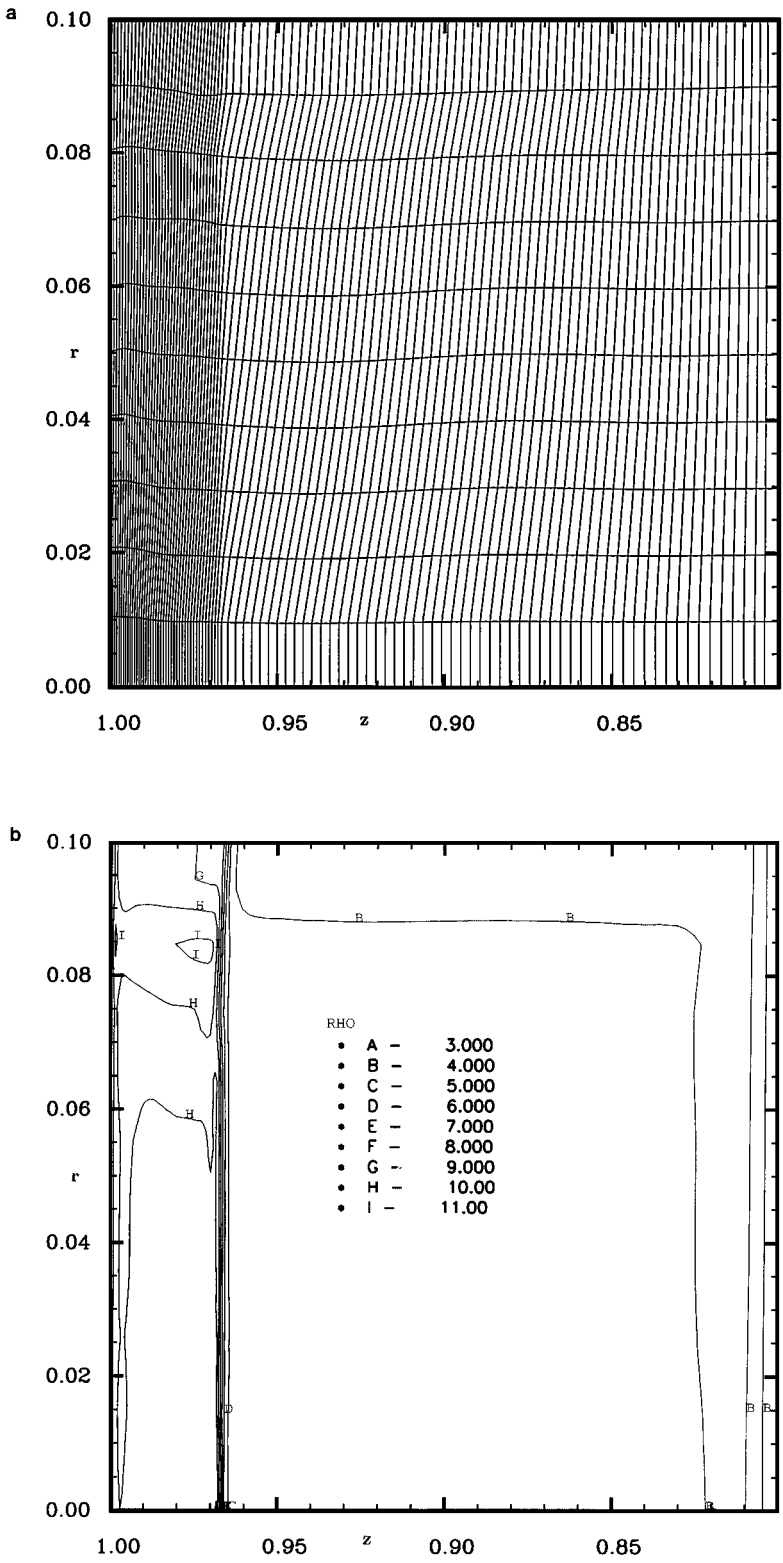

FIG. 6. (a) Saltzman piston problem. Grid at $t = 0.80$ with original gradient operator. (b) Saltzman piston problem. Contour plot of density at $t = 0.80$ with original gradient operator. (c) Saltzman piston problem. Grid at $t = 0.80$ with new gradient operator. (d) Saltzman piston problem. Contour plot of density at $t = 0.80$ with new gradient operator.

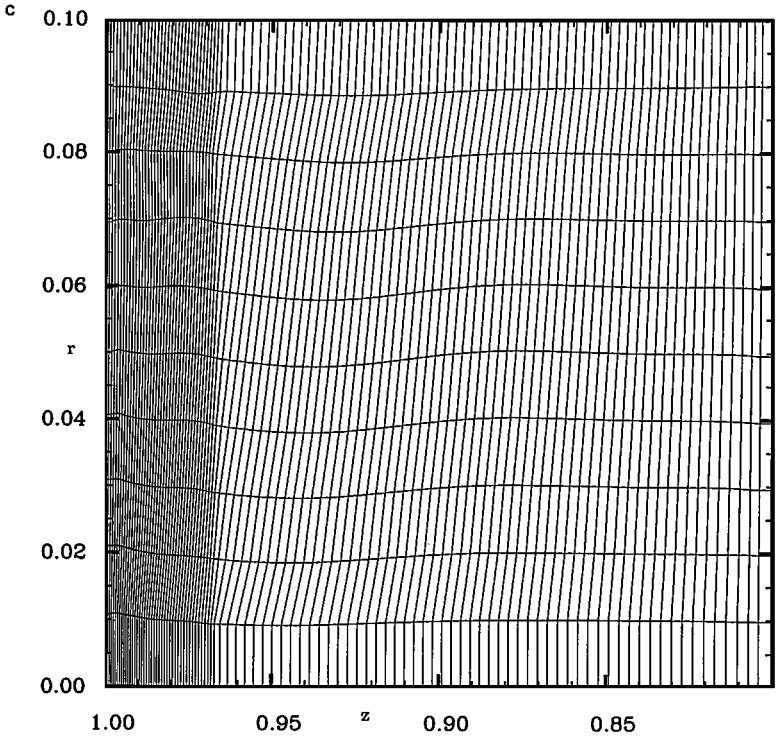

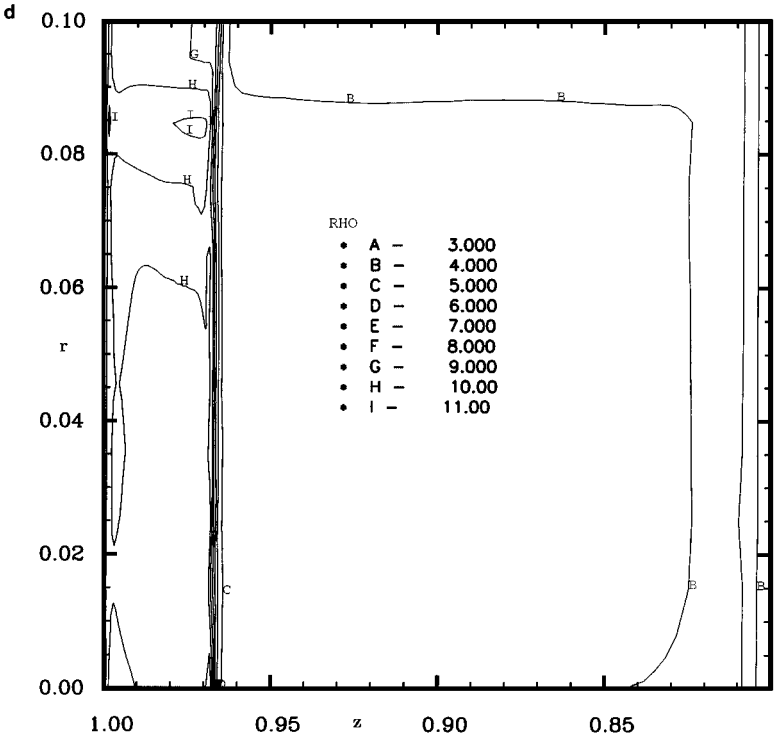

FIG. 6—*Continued*

5.1. *Conservation of momentum.* We first demonstrate conservation of momentum for control volume differencing and then show that both the modified gradient operator and area-weight differencing do not strictly conserve linear momentum. This is most easily done by considering pressure forces constructed with respect to the median mesh. Consider the piece of force $P_0\mathbf{S}_1$ in Fig. 2. This acts with a minus sign on point "*c*" and with a plus sign on point "*a*" for a control volume scheme. Thus, momentum conservation stated as the requirement that the sum of all nodal forces be equal to the applied boundary force is trivially satisfied for control volume differencing. Since the coordinate-line and median meshes are identical for control volume differencing the pressure forces can be computed along the coordinate-line mesh just as well and momentum is still conserved. What has been shown is that momentum is conserved for a constant zone pressure, P_0, as long as the associated zone is defined by a "closed" boundary, since then the total force due to that pressure (but distributed amongst all of its defining points) is $P_0 \int d\mathbf{S} \equiv 0$. When we modify the lengths $\mathbf{a}_i$ of the coordinate-line mesh to obtain symmetry the sum of these vectors about a given zone no longer add to zero. Therefore, the zone is not closed; momentum is thus no longer exactly conserved; and the new coordinate-line mesh is not equivalent to the median mesh. A point that seems to have been missed by the originators of the various forms of the area-weight schemes is that for these schemes momentum conservation is also not satisfied. This is easily seen from the fact that in Fig. 2 the force on point "*c*" is $-P_0 r_c \mathbf{S}_1$, while that on point "*a*" is $+P_0 r_a \mathbf{S}_1$. The different factors of "*r*" break the momentum balance. The new gradient operator also breaks the momentum balance with respect to the usual control volume scheme, where previously it was exact.

It is easy to measure the magnitude of this numerical error in the case where there are no applied boundary forces by computing the total linear momentum in the "*z*" direction, which is easily defined unambiguously in cylindrical geometry. To this end we define the defect in linear momentum conservation, δL_m, as the sum over all points of the total force in the *z* direction divided by the sum of its magnitude, viz.

$$\delta L_m = \sum_p (\mathbf{F}_p \cdot \hat{z}) \Big/ \sum_p |\mathbf{F}_p \cdot \hat{z}|. \tag{19}$$

For the Lazarus problem shown in Fig. 3b that is run with the original, unmodified control volume differencing $\delta L_m \sim 10^{-15}$ until the run terminates due to excessive grid distortion. For this problem run with control volume differencing using the modified gradient operator or with area-weight differencing, both with equal angle zoning as given by Fig. 3c and Fig. 3a, respectively, $\delta L_m \sim 10^{-3}$ for both schemes. With increased angular resolution this quantity decays in magnitude as the truncation error of a scheme with approximately second-order accuracy. For unequal angle zoning, as shown in Fig. 4c, δL_m is somewhat larger for either scheme. For the aspherical expansion problem $\delta L_m \sim 10^{-4}$ for both schemes shown. Although the defect in momentum conservation is usually roughly equal in both schemes (by factors of three or so), in the Sedov blast wave problem [5, 17], where all the energy is initially concentrated in a single zone on an initially square grid δL_m can be as large as a few percentages at the early part of the run, decaying to much less that 1% at the end with area-weight differencing. In this instance it is much larger (10 or so) for the area-weight scheme, relative to the control volume scheme with modified gradient operator. This is due to the fact that the initial energy is concentrated where $\Delta r/r$ is large; modified area-weight differencing is more explicitly sensitive to this quantity than is modified control volume

differencing, although it is the size of this term that largely determines the nonconservation of momentum in both cases. The differences in results (density, pressure, etc.) between these two schemes and standard control volume differencing is still very small in this instance, where no symmetry relative to the grid orientation is present. We thus conclude that this lack of exact conservation of linear momentum, although somewhat paradoxical, does not cause serious damage to the results when symmetry is not present. In fact, it is curious that this appears to be necessary in order to obtain good results when symmetry should be present or nearly so. That is, it seems to be necessary to violate conservation of linear momentum at truncation error levels in order to inhibit the production of totally unphysical angular momentum that can completely destroy the solution.

6. CONCLUSIONS

In this work we have shown how the problem of exactly preserving numerically a one-dimensional symmetry, in a two-dimensional coordinate system distinct from that symmetry, can be achieved for a wide range of initial grids, and without necessarily resorting to very specialized finite difference schemes. It was shown that this could be attained through a modification of the pressure gradient operator. This modification, motivated by a circle construction through three points, led to a very effective and simple to implement prescription for slightly changing this operator to detect cylindrical and spherical symmetry in Cartesian and cylindrical geometry, respectively, when present in the initial and boundary conditions. The effectiveness of this new gradient operator was shown with numerical examples. For problems without any symmetry it was shown that the new gradient operator produced very little difference from the original form, thus demostrating that this prescription is useful for perturbation studies.

APPENDIX A: FORCES DERIVING FROM A TENSOR

The procedure developed in Section 3 has been shown to be effective in preserving symmetry with pressure forces. Here we briefly discuss the case where the force is derived from the divergence of a tensor, $\mathbf{T}$, as occurs in solving problems involving material strength. The momentum equation in Lagrangian form is now given as $\rho\, d\mathbf{v}/dt = \nabla\cdot\mathbf{T}$, which written in component form in two-dimensional, cylindrical geometry becomes

$$\rho\frac{dv_r}{dt} = \frac{\partial T_{rr}}{\partial r} + \frac{\partial T_{rz}}{\partial z} + \frac{(2T_{rr} - T_{zz})}{r}, \tag{20}$$

$$\rho\frac{dv_z}{dt} = \frac{\partial T_{rz}}{\partial r} + \frac{\partial T_{zz}}{\partial z} + \frac{T_{rz}}{r}. \tag{21}$$

A tensor that gives rise to symmetric motion has components that transform from one angular location to another along an l-line by means of a rotation matrix. This is equivalent to the pressure being constant on a given side of each l-line as shown in Fig. 1. The rotation matrix that effects this transformation through an arbitrary angle ψ is given by

$$\mathbf{C} = \begin{bmatrix} \cos\psi & \sin\psi \\ -\sin\psi & \cos\psi \end{bmatrix}, \tag{22}$$

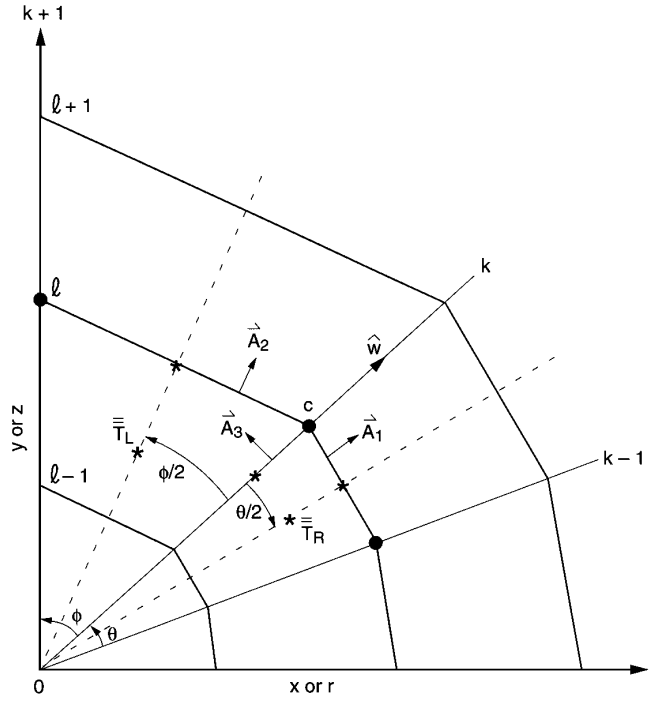

FIG. 7. Unequal angle grid for force calculation as the divergence of a tensor. Tensors $\mathbf{T}_L$ and $\mathbf{T}_R$ are defined at centers of zones that lie to the left and right of the line labelled "*k*", and below line "*l*".

where the matrix $\mathbf{T}$ that is acts upon is defined at zone center points whose coordinates are given as the average of the coordinates of the points that define the zone. If in two-dimensions the matrix $\mathbf{T}$ is made diagonal at some location, say along the line labelled "*k*" in Fig. 7, with entries denoted by $T_\parallel$ and $T_\perp$ along the diagonal with respect to the direction of the unit vector defined as $\hat{w}$ in Section 3, then this matrix when rotated through an angle ψ is given by $\mathbf{C}^{-1}\mathbf{T}\mathbf{C}$. Using dyadic notation this has the form

$$\mathbf{C}^{-1}\mathbf{T}\mathbf{C} = \begin{bmatrix} (T_\parallel \cos^2\psi + T_\perp \sin^2\psi)\hat{w}\hat{w} & \left(\frac{T_\parallel - T_\perp}{2}\right)\sin(2\psi)\hat{w}\hat{w}_\perp \\ \left(\frac{T_\parallel - T_\perp}{2}\right)\sin(2\psi)\hat{w}_\perp\hat{w} & (T_\parallel \sin^2\psi + T_\perp \cos^2\psi)\hat{w}_\perp\hat{w}_\perp \end{bmatrix}, \quad (23)$$

where in this representation $\hat{w} = (1, 0)$ and $\hat{w}_\perp = (0, 1)$.

Next, consider the symmetric situation as shown in Fig. 7, where the tensor $\mathbf{T}_L$ defined in the center of the zone that lies on the lower left side of point "*c*" is obtained from Eq. (23) by setting $\psi = \phi/2$; the tensor $\mathbf{T}_R$ is defined in the center of the zone lying to the lower right side of this point and is obtained by setting $\psi = -\theta/2$ in Eq. (23). From the notation given in Fig. 7, the discrete force that arises from these two tensors acting on point "*c*" in the case of Cartesian geometry (when the hoop stress terms in Eqs. (20), (21) are set to zero) for control volume differencing of the derivative terms in Eqs. (20), (21), denoted as $\mathbf{F}_{g,l}$, can be written as $\mathbf{F}_{g,l} \equiv \mathbf{T}_L \cdot (\mathbf{A}_2 - \mathbf{A}_3) + \mathbf{T}_R \cdot (\mathbf{A}_1 + \mathbf{A}_3)$. Defining the vectors $\mathbf{A}_1 = (a_1^\parallel, a_1^\perp)$, $\mathbf{A}_2 = (a_2^\parallel, a_2^\perp)$, and $\mathbf{A}_3 = (0, a_3^\perp)$ as shown in Fig. 7

with respect to the directions $\hat{w}$ and $\hat{w}_\perp$ this equation for the force when expanded out in full is

$$\begin{aligned}
\mathbf{F}_{g,l} = &\left[(T_\parallel \cos^2(\phi/2) + T_\perp \sin^2(\phi/2))a_2^\parallel + \left(\frac{T_\parallel - T_\perp}{2}\right)(\sin\phi)a_2^\perp\right]\hat{w} \\
&+ \left[\left(\frac{T_\parallel - T_\perp}{2}\right)(\sin\phi)a_2^\parallel + (T_\parallel \sin^2(\phi/2) + T_\perp \cos^2(\phi/2))a_2^\perp\right]\hat{w}_\perp \\
&- \left[\left(\frac{T_\parallel - T_\perp}{2}\right)(\sin\phi)a_3^\perp\right]\hat{w} - \left[(T_\parallel \sin^2(\phi/2) + T_\perp \cos^2(\phi/2))a_3^\perp\right]\hat{w}_\perp \\
&+ \left[(T_\parallel \cos^2(\theta/2) + T_\perp \sin^2(\theta/2))a_1^\parallel - \left(\frac{T_\parallel - T_\perp}{2}\right)(\sin\theta)a_1^\perp\right]\hat{w} \\
&+ \left[-\left(\frac{T_\parallel - T_\perp}{2}\right)(\sin\theta)a_1^\parallel + (T_\parallel \sin^2(\theta/2) + T_\perp \cos^2(\theta/2))a_1^\perp\right]\hat{w}_\perp \\
&- \left[\left(\frac{T_\parallel - T_\perp}{2}\right)(\sin\theta)a_3^\perp\right]\hat{w} + \left[(T_\parallel \sin^2(\theta/2) + T_\perp \cos^2(\theta/2))a_3^\perp\right]\hat{w}_\perp. \quad (24)
\end{aligned}$$

From the preceeding equation we separate and rearrange all terms that are in the direction $\hat{w}_\perp$, that is perpendicular to the symmetry direction $\hat{w}$, and which must therefore vanish if symmetry is to be preserved. This yields

$$\begin{aligned}
F_{g,l\perp} = &\left[(T_\parallel \sin^2(\phi/2) + T_\perp \cos^2(\phi/2))a_2^\perp + (T_\parallel \sin^2(\theta/2) + T_\perp \cos^2(\theta/2))a_1^\perp\right] \\
&+ a_3^\perp\left[T_\parallel(\sin^2(\theta/2) - \sin^2(\phi/2)) + T_\perp(\cos^2(\theta/2) - \cos^2(\phi/2))\right] \\
&+ \left(\frac{T_\parallel - T_\perp}{2}\right)\left(a_2^\parallel \sin\phi - a_1^\parallel \sin\theta\right). \quad (25)
\end{aligned}$$

The expression given by Eq. (25) allows a number of interesting limits to be examined. First, when we have only pressure forces $T_\parallel = T_\perp \equiv -P$, then the last two lines on the RHS of Eq. (25) vanish, while the first line reduces to $-P(a_2^\perp + a_1^\perp)$ so that all angular factors have disappeared. As was noted in Section 3 and can be seen from Fig. 7, the lengths $a_1^\perp$ and $a_2^\perp$ always have opposite signs; the procedure, given by Eqs. (12), (13), makes their magnitudes equal when they would not be so otherwise and, thus, symmetry is obtained for forces that arise from a symmetric distribution of pressure. Next, suppose that $\phi = \theta$, equal angle zoning. Then for $T_\parallel \neq T_\perp$ it is seen that Eq. (25) vanishes if and only if $a_2^\perp = -a_1^\perp$ and $a_2^\parallel = a_1^\parallel$. This occurs only for a control volume scheme in Cartesian geometry or an area-weight scheme in cylindrical geometry with equal angle zoning. In the latter case the hoop stress terms in Eqs. (20), (21) that appear as momentum sources can be added to the discrete force by defining the divisor "r" that appears in them at the zone centers and then area weighting these terms to their surrounding dynamical points by the associated subzonal corner area. In this case symmetry will still be obtained [18].

For unequal angle zoning the terms in Eq. (25) do not cancel in any simply arranged manner. To remedy this situation we employ the following procedure. First, we utilize the symmetry direction $\hat{w}$ as defined by Eq. (8), but only along lines that are assumed apriori to potentially form level lines of the symmetric solution [these are the l-lines of Fig. (7)]. Then with respect to these lines only we modify the forces that arise from

the now assumed traceless tensor $\mathbf{T}$ in a manner completely analogous to that given by Eqs. (9–13) for the half-edge coordinate line vectors. Referring to Fig. (7) we define $\mathbf{F}_L^T$ and $\mathbf{F}_R^T$ as forces that originate from the tensors $\mathbf{T}_L$ and $\mathbf{T}_R$ and act on point "c". (In the case of cylindrical geometry the hoop stress terms are included.) We next define $\mathbf{F}_{\perp,L}^T$ and $\mathbf{F}_{\perp,R}^T$ as the components of these forces that are perpendicular to $\hat{w}$, where $\hat{w}$ is defined at point "c" by Eq. (8) along line "l". These perpendicular forces are then averaged to define $\mathbf{F}_\perp^T$ taking into account the fact that they lie in opposite directions. This can be expressed as

$$\begin{aligned} \mathbf{F}_{\perp,L}^T &\equiv \mathbf{F}_L^T - \left(\mathbf{F}_L^T \cdot \hat{w}\right)\hat{w}, \\ \mathbf{F}_{\perp,R}^T &\equiv \mathbf{F}_R^T - \left(\mathbf{F}_R^T \cdot \hat{w}\right)\hat{w}, \\ \mathbf{F}_\perp^T &= \left(\mathbf{F}_{\perp,L}^T - \mathbf{F}_{\perp,R}^T\right)/2. \end{aligned} \tag{26}$$

Next we construct the new forces that act on point "c" from adjacent zones on the same side of a common l-line by using the newly defined $\mathbf{F}_\perp^T$ along with the unchanged component of the force in the $\hat{w}$ direction. This yields for these new forces the result

$$\mathbf{F}_L^{TM} = \left(\mathbf{F}_L^T \cdot \hat{w}\right)\hat{w} + \mathbf{F}_\perp^T, \tag{27}$$

$$\mathbf{F}_R^{TM} = \left(\mathbf{F}_R^T \cdot \hat{w}\right)\hat{w} - \mathbf{F}_\perp^T, \tag{28}$$

where the superscript "M" indicates the modified forces that are actually employed in the discrete from of the momentum equation.

The above procedure does not guarantee that symmetry will be preserved when it is present in the spatial distribution of the tensor $\mathbf{T}$. For this to be true it is required in addition that both the acceleration and the heating rate be constant in magnitude along an l-line, as discussed previously. We find in numerical simulations in two dimensions that for control volume differencing in Cartesian geometry or area-weight differencing in cylindrical geometry that the above procedure results in symmetry preservation to roundoff error for unequal angle initial zoning. This is in addition to the case of equal angle zoning where it is, of course, unnecessary. In the case of control volume differencing in cylindrical geometry the magnitude of the acceleration along an l-line is not found to be constant except for equal angle initial zoning. In this instance it is observed that errors in symmetry arise slowly near the "z" axis where $\Delta r/r$ is of order unity. As a result symmetry is lost everywhere after a few hundreds of cycles.

ACKNOWLEDGMENTS

We thank D. E. Burton, L. G. Margolin, and M. J. Shashkov for useful and interesting discussions of this subject.

REFERENCES

1. M. L. Wilkins, Calculations of elastic-plastic flow, *Methods Comput. Phys.* **3**, 211 (1964).
2. W. D. Schulz, Two-dimensional Lagrangian hydrodynamic difference equations, *Methods Comput. Phys.* **3**, 1 (1964).
3. V. F. Tishkin, N. N. Tiurina, and A. P. Favorskii, *Finite-Difference Schemes for Calculating Hydrodynamic Flows in Cylindrical Coordinates*, Preprint No. 23, Institute of Applied Mathematics, Moscow, Russia, 1978.

4. P. P. Whalen, Algebraic limitations on two-dimensional hydrodynamics simulations, *J. Comput. Phys.* **124**, 46 (1996).
5. E. J. Caramana, D. E. Burton, M. J. Shashkov, and P. P. Whalen, The development of compatible, mimetic, hydrodynamics algorithms utilizing conservation of total energy, *J. Comput. Phys.*, submitted.
6. P. L. Browne, *Integrated Gradients: A Derivation of Some Difference Forms for the Equation of Motion for Compressible Flow in Two-Dimensional Lagrangian Hydrodynamics*, Los Alamos National Laboratory Report LA-10587-MS (1986).
7. G. D. Simonov, Using the model of a thin deforming shell for generation and analysis of 2-D gas dynamics, *Mat. Modelir Fiz. Proc.* **3**, 41 (1993). [Questions of Atomic Structure and Technology-Mathematical Modeling of Physical Processes]
8. L. G. Margolin and J. J. Pyun, *A method for Treating Hourglass Patterns*, Los National Laboratory Report LAUR-87-439 (1987).
9. E. J. Caramana and M. J. Shashkov, The elimination of spurious vorticity, grid tangling, and hourglass-type motions by means of Lagrangian subzonal masses and pressures, *J. Comp. Phys.*, submitted.
10. M. L. Wilkins, Use of artificial viscosity in multidimensional fluid dynamic calculations, *J. Comp. Phys.* **36**, 281 (1980).
11. E. J. Caramana, M. J. Shashkov, and P. P. Whalen, An edge-centered artificial viscosity for multi-dimensional shock wave computations, *J. Comp. Phys.*, submitted.
12. R. Lazarus, Self-similar solutions for converging shocks and collapsing cavities, *SIAM J. Numer. Anal.* **18**, 316 (1981).
13. G. Guderley, Starke kugelige und zylindrische Verdichtungsstosse in der Nahe des Kugelmittelspunktes bzw. der Zylinderachse, *Luftfahrt-Forsch.* **19**, 302 (1942).
14. K. P. Stanyukovich, *Unsteady Motion of Continuous Media* (Academic Press, New York, 1960), p. 506.
15. F. J. Dyson, *Free Expansion of a Gas 2, Gaussian Model*, John Jay Hopkins Laboratory report GAMD-507 (1958).
16. J. K. Dukowicz and B. Meltz, Vorticity errors in multidimensional Lagrangian codes, *J. Comp. Phys.* **99**, 115 (1992).
17. L. I. Sedov, *Similarity and Dimensional Methods in Mechanics* (Academic Press, New York, 1959).
18. D. E. Burton, *Multidimensional Discretization of Conservation Laws for Unstructured Polyhedral Grids*, Lawrence Livermore National Laboratory report UCRL-53882 (1994).